Author/s:
Zhang, J;Cao, J;Zheng, R;Yu, M;Lin, Z;Wang, C;McCluskey, J;Yang, J;Chen, Z;Corbett, AJ;Cao, P;Mo, W;Wang, Z

Title:
The establishment of a cytomegalovirus -specific CD8+ T-cell threshold by kinetic modeling for the prediction of post-hemopoietic stem cell transplant reactivation

Date:
2022-11-18

Citation:
Zhang, J., Cao, J., Zheng, R., Yu, M., Lin, Z., Wang, C., McCluskey, J., Yang, J., Chen, Z., Corbett, A. J., Cao, P., Mo, W. & Wang, Z. (2022). The establishment of a cytomegalovirus -specific CD8+ T-cell threshold by kinetic modeling for the prediction of post-hemopoietic stem cell transplant reactivation. Iscience, 25 (11), https://doi.org/10.1016/j.isci.2022.105340.

Persistent Link:
https://hdl.handle.net/11343/335101

iScience

CellPress
OPEN ACCESS

Article

The establishment of a cytomegalovirus -specific CD8$^+$ T-cell threshold by kinetic modeling for the prediction of post-hemopoietic stem cell transplant reactivation

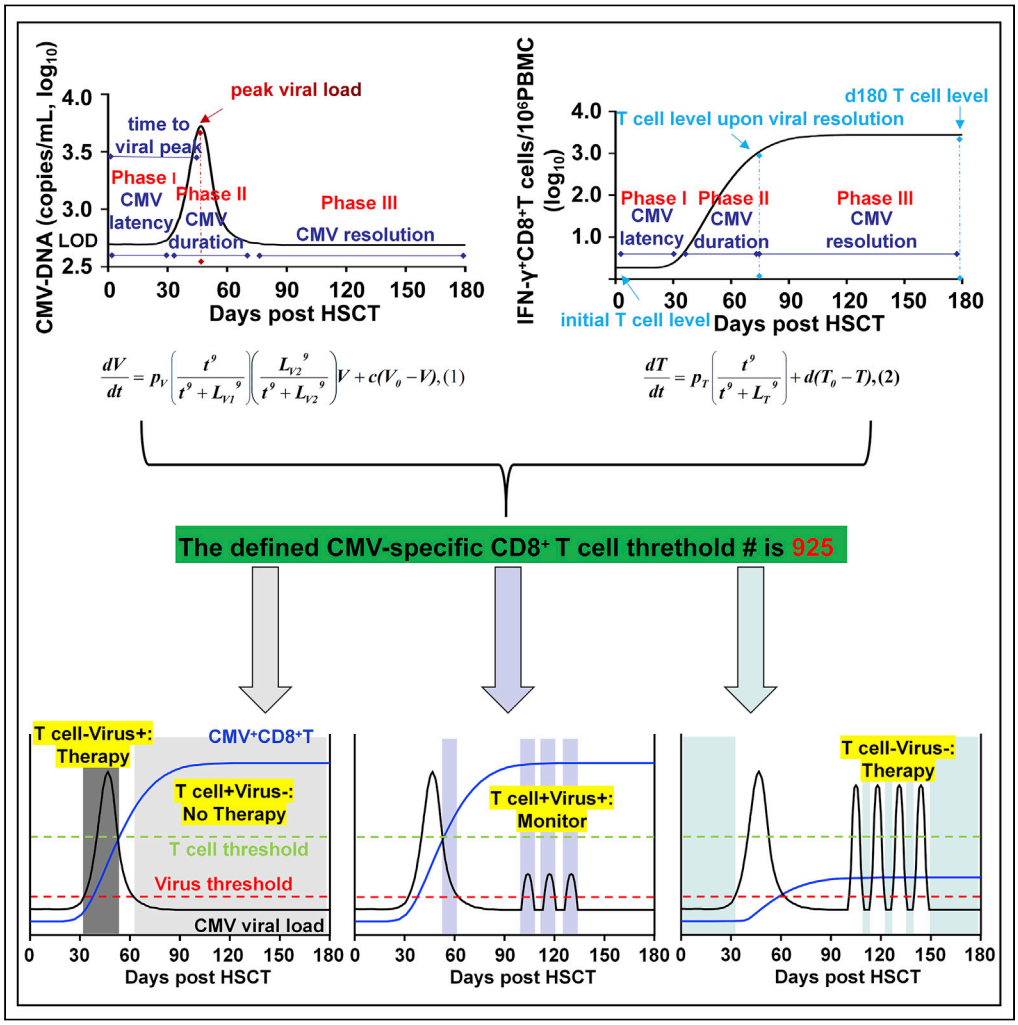

Jing Zhang, Jinpeng Cao, Runhui Zheng, ..., Pengxing Cao, Wenjian Mo, Zhongfang Wang

corbetta@unimelb.edu.au (A.J.C.)
pengxing.cao@unimelb.edu.au (P.C.)
eywjmo@scut.edu.cn (W.M.)
wangzhongfang@gird.cn (Z.W.)

Highlights

CMV reactivation and tailored specific T-cell response kinetics were established

CMV reactivation started at d25 (d17-d35) and last for 51 (33–63) days

CMV-specific CD8$^+$ T cells are responsible for suppressing CMV reactivation

CMV-specific CD8$^+$ T-Threshold was defined as 925/10^6 PBMC

Zhang et al., iScience 25, 105340
November 18, 2022
https://doi.org/10.1016/j.isci.2022.105340

iScience

CellPress
OPEN ACCESS

Article

The establishment of a cytomegalovirus -specific CD8$^+$ T-cell threshold by kinetic modeling for the prediction of post-hemopoietic stem cell transplant reactivation

Jing Zhang,[1,2,7] Jinpeng Cao,[1,2,7] Runhui Zheng,[3,7] Mengqiu Yu,[1,7] Zhengfang Lin,[1,7] Caixia Wang,[4] James McCluskey,[5] Ji Yang,[1] Zhenjun Chen,[5] Alexandra J. Corbett,[5,*] Pengxing Cao,[6,*] Wenjian Mo,[4,*] and Zhongfang Wang[1,2,8,*]

SUMMARY

The dynamic interaction between the CMV virus and host immune response remains obscure, thus hindering the diagnosis and therapeutic management of patients with HSCT. The current diagnosis of CMV viremia depends on viral load estimation. Medical intervention based on viral load, can be unnecessary or poorly timed for many patients. Here we examined the clinical features and blood samples of patients with HSCT and assessed the CMV reactivation kinetics and corresponding CMV antigen-specific T-cell response in individual patients based on a peptide pool stimulation T-cell assay, which showed that CMV-specific CD8$^+$ T cells were more suitable to be a diagnosis indicator for suppressing CMV reactivation. Using ROC analysis, we defined and verified a CMV-specific CD8$^+$ T-cell counts threshold (925 cells/10^6 PBMCs) as an indicator of CMV reactivation post-HSCT, and suggested that use of this threshold would provide more accurate guidance for prompt medication and better management of CMV infection post-HSCT.

INTRODUCTION

Cytomegalovirus (CMV) infection is one of the major causes of morbidity and mortality following allogeneic hemopoietic stem cell transplant (HSCT), which is used to treat a variety of blood disorders, including non-malignant diseases, e.g., aplastic anemia, and hematologic malignancy, e.g., leukemia, lymphoma and multiple myeloma (de Koning et al., 2016; Simons et al., 2019). For a period of time after HSCT, recipients' immunity remains depleted and suppressed while the reconstitution of donor-derived host immunity is in progress, leaving HSCT recipients vulnerable to opportunistic infections. Indeed, at this stage, pre-existing latent CMV from the host or graft can flare up within the recipient (Liu et al., 2015; Moss and Rickinson, 2005). It is known that CMV reactivation occurs in approximately 60% to 70% of seropositive patients with HSCT within the first 100 days post-HSCT, and without prompt additional viral suppression treatment up to 10% of patients progress into potentially fatal CMV diseases which include pneumonitis, gastritis, enteritis, colitis, hepatitis, retinitis, and encephalitis (Boeckh et al., 2003; Einsele et al., 2020; Goldsmith et al., 2016; Hodowanec et al., 2020; Lee et al., 2017; Maertens and Lyon, 2017).

Currently, CMV reactivation is diagnosed through the estimation of blood CMV titer by CMV-DNA and -antigen (pp65) tests (Berth et al., 2016; Kamei et al., 2016). However, these snapshots of blood viral load are far from satisfactory for the clinical assessment of overall disease severity or prediction of disease outcomes. A CMV-DNA positive result does not always manifest any CMV disease, whereas a negative CMV-DNA result cannot rule out the development of CMV diseases. Consequently, in the hospitals of our study cohort, a 3-month prophylactic antiviral therapy with antiviral agents (ganciclovir, valganciclovir or foscarnet) is routinely applied following HSCT to reduce the chance of CMV recurrence (Boeckh and Ljungman, 2009; Sellar and Peggs, 2012). Then, pre-emptive approach after the first 90 days is performed involving close viral load monitoring and antiviral treatment for significant viral reactivation. However, the prolonged use of these antiviral drugs can cause adverse effects on bone marrow and kidneys and may lead to the selection of drug-resistant strains of CMV (Boeckh and Ljungman, 2009; Heagy et al., 1991; Ljungman

[1]State Key Laboratory of Respiratory Disease & National Clinical Research Center for Respiratory Disease, Guangzhou Institute of Respiratory Health, the First Affiliated Hospital of Guangzhou Medical University, Guangzhou Medical University, Guangzhou, China

[2]Guangzhou Laboratory, Bio-Island, Guangzhou, China

[3]Department of Hematology, the First Affiliated Hospital of Guangzhou Medical University, Guangzhou Medical University, Guangzhou, China

[4]Department of Hematology, Guangzhou First People's Hospital, School of Medicine, South China University of Technology, Guangzhou, China

[5]Department of Microbiology and Immunology, Peter Doherty Institute for Infection and Immunity, The University of Melbourne, Melbourne, VIC 3000, Australia

[6]School of Mathematics and Statistics, The University of Melbourne, Melbourne, VIC 3010, Australia

[7]These authors contributed equally

[8]Lead contact

*Correspondence: corbetta@unimelb.edu.au (A.J.C.), pengxing.cao@unimelb.edu.au (P.C.), eywjmo@scut.edu.cn (W.M.), wangzhongfang@gird.cn (Z.W.)

https://doi.org/10.1016/j.isci.2022.105340

et al., 2010). Moreover, the high costs of anti-viral therapy impose a huge financial burden on patients whose medical costs are not fully covered by insurance. Thus, from a clinical perspective, there is an urgent need to develop improved diagnostic methods to monitor CMV reactivation and guide targeted antiviral therapy.

Previous studies, in a mouse model and in human HSCT cases, have shown that $CD8^+$ T-cells, $CD4^+$ T-cells, natural killer (NK) cells, and B cells all play important roles in controlling CMV reactivation (Alegre, 2019; Apiwattanakul et al., 2020; Chang et al., 2014; Rogers et al., 2020). However, the reconstitution of recipients' adaptive immunity through the engraftment of donor stem cells is a slow process, which occurs over months to years (van den Brink et al., 2015). In addition, the re-establishment of host immunity can be affected by multiple HSCT-related factors such as recipient and donor CMV serostatus, the stem cell source, the degree of human-leukocyte-antigen (HLA) matching, infections, presence of graft-versus-host disease (GVHD) and degree of corticosteroids use for immune suppression (Pei et al., 2017). The variations of these factors in individual patients make it difficult to accurately evaluate the true extent of immune reconstitution after HSCT. To date, no standardized index or threshold has been established to indicate an effective immunity for controlling CMV reactivation (Camargo et al., 2019; Tey et al., 2013). Furthermore, during the immune reconstitution, fluctuations of recipients' immunity occur frequently, which may allow CMV recurrence. Therefore, a better understanding of the dynamic relationship between host immune responses, particularly T-cell immunity, and CMV reactivation is important for better management of post-HSCT CMV-mediated complications (Wagner-Drouet et al., 2021).

In this study, we analyzed blood samples of 88 patients from Guangzhou First People's Hospital (GFPH) and 43 patients from the First Affiliated Hospital of Guangzhou Medical University (GMUH) who had undergone HSCT. CMV-specific T-cell immunity ($CD4^+$ and $CD8^+$) assays were performed based on a peptide pool stimulation T-cell assay and CMV titers were measured (via DNA) at various timepoints over a period of 90 days to 3 years post-HSCT. Reiterative computational data-fitting allowed us to develop a mathematical model through which a significant correlation was established between CMV reactivation kinetics and the antigen-specific $CD8^+$ T-cell response. Importantly, by analysis of patients from two different hospitals, we were able to define a threshold of CMV-specific $CD8^+$ T-cell counts (per million PBMCs) that corresponded, in most cases, to CMV containment. We then verified the use and robustness of the threshold in separate patient cohorts. Thus, we defined a new parameter: CMV-specific $CD8^+$ T-cell counts per million PBMCs, which has the potential to be used as an effective cue for anti-viral therapy.

RESULTS

Clinical characteristics of patients and incidence of cytomegalovirus viremia following hemopoietic stem cell transplant

In this study, two cohorts of patients with HSCT, diagnosed with acquired severe aplastic anemia (SAA) (cohort I: 64 patients) and hematologic malignancy (HM) (cohort II: 24 patients), respectively, were recruited from Guangzhou First People's Hospital (GFPH), the largest SAA diagnosis and treatment center in South China (Table 1). Additionally, 21 patients with HSCT, each diagnosed with various forms of HM, were recruited from a different hospital, the First Affiliated Hospital of Guangzhou Medical University (GMUH) (Cohort III, Table 1). The clinical characteristics of the patients, including donor source, stem cell source, donor/recipient CMV serostatus, and the presence or absence of GVHD, were summarized in Table 1.

To analyze CMV-DNAemia occurrence in the three cohorts, we performed quantitative real-time PCR using plasma collected at various timepoints between 2 weeks before and 3 years after HSCT. The diagnostic criterion of CMV viremia was defined as 500 copies/mL in plasma (clinical threshold for treating). Based on the medical records and laboratory data, the occurrence of viremia over time was assessed. For the patient cohorts from GFPH, the accumulative CMV incidences were 80.3% (74.7% at d60) and 61.4% (47.8% at d60) for HSCT patients with SAA (cohort I) and HM (cohort II), respectively (Figures S1A and S1B). For cohort III (patients with HM from GMUH), the overall cumulative CMV incidence was 61.7% (51.3% at d60) (Figure S1C), similar to that of cohort II ($p = 0.8443$). Collectively, these results show that the incidence of CMV reactivation rises rapidly before d60 and reaches a plateau at around d100, in agreement with previous clinical observations (Green et al., 2012, 2013).

Table 1. Characteristics of study subjects

Medical center	GFPU		GMUH
Cohort	I (n = 64)	II (n = 24)	III (n = 21)
Median age, years (range)	28.5 (9–57)	39 (16–62)	32(19–65)
Sex			
Males	34	17	14
Females	30	7	7
Diagnosis			
SAA (severe aplastic anemia)	64		
MDS (myelodysplastic syndrome)		6	2
ALL (acute lymphoctic leukemia)		5	7
AML (acute myeloid leukemia)		10	6
PCL (plasma cell leukemia)		2	1
TL (T lymphoma)		1	1
BL (B lymphoma)			1
NKL (NK lymphocytic leukemia)			2
HLH (hemophagocytic lymphohistiocytosis)			1
Donor source			
HID (haplo-identical donor)	24	13	17
MSD (matched sibling donor)	23	5	4
URD (unrelated donor)	17	6	
Stem cell source			
Peripheral blood	17	6	3
Peripheral blood + Bone marrow	47	18	18
CMV donor/recipient srostatus			
D + R+	64	24	21
GVHD, any	8	9	17
Grade II-IV	7	9	10
Number of deaths	4	7	4
Death from relapse		4	3
Non-relapse death	4	3	1
CMV reactivation in observation period, any	49	15	21
CMV viremia	49	14	21
CMV enteritis	1		
CMV retinitis	6	3	

Dynamic distribution of cytomegalovirus loads in patients following hemopoietic stem cell transplant

The large set of PCR data (1775 samples from 88 patients) obtained from the GFPH cohorts (I & II) allowed us to investigate the kinetics of CMV reactivation. We first produced a heat map for both patients with SAA and HM that displays the distribution and level of CMV viremia over a period of 330 days (Figure 1A). A very low CMV incidence was seen within the first 30 days after HSCT (Figures 1A and 1B). This was followed by a large increase in the detection of CMV between d30-60. After d60, the incidence of CMV detection declined (Figures 1A and 1B).

To further analyze the dynamic distribution of CMV viral loads, we selected patients who had one episode of CMV reactivation within 90 days post-HSCT (43 from the 88 patients) (Figure 1C) and fitted their DNA data into a single ordinary differential equation (for details see STAR methods). After reiterate computational modeling, a representative CMV-DNA kinetic curve was generated (Figure 1D) from the data of individual cases (Figure S2). Consistent with our conclusions from the heat map visualization, the bulk of CMV

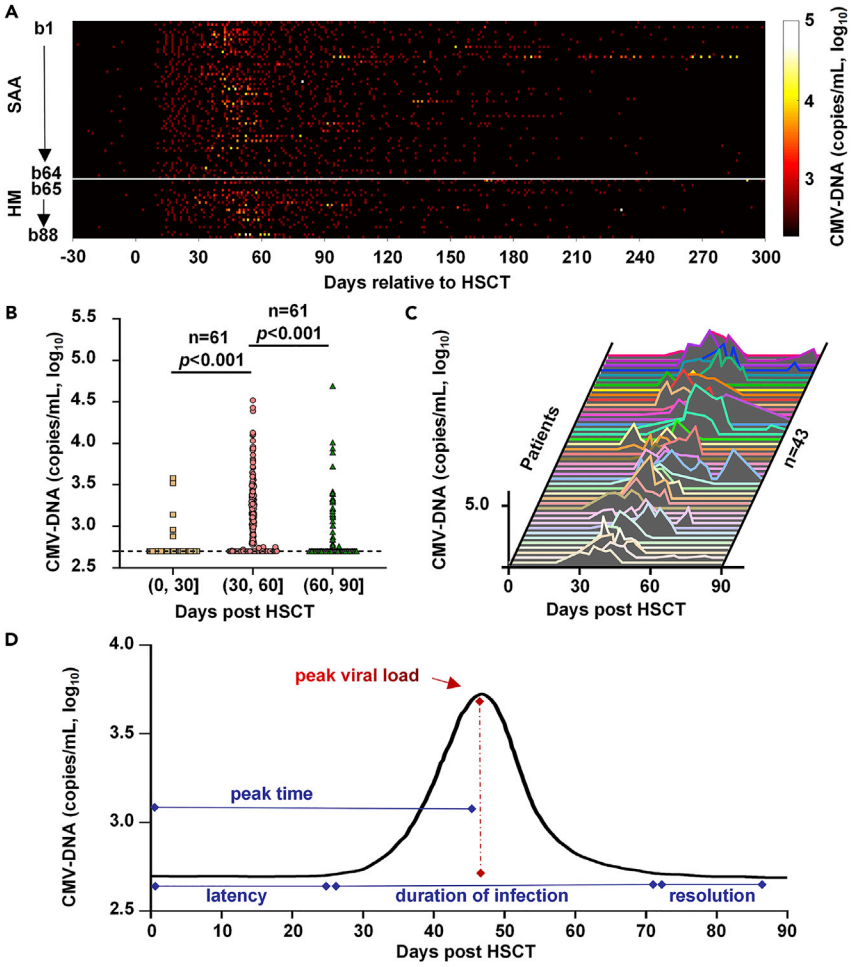

E

CMV infection (re-activation)	Estimate median & (min-max)
peak viral load	2403.4 (958.2—30551.0)
peak time (days)	44 (29—64)
latency (days)	25 (17—35)
duration of infection (days)	51 (33—63)

Figure 1. Observed and modeled CMV load kinetics

(A) A heatmap generated using the viral load data (CMV copies per mL plasma) over the period of 330 days from 88 patients with HSCT, including 64 SAA (top section) and 24 HM (bottom section) cases. The data are displayed with a color-coded scale from undetectable level (black dots, same as the background, $\leq$500 copies per mL of plasma) to $\geq 10^5$ copies per mL of plasma (white dots). X-axis represents time relative to HSCT.

(B) CMV viral-load data (in $\log_{10}$ scale) in three time-period divisions (d0-30, d30-60, and d60-90) generated by a likelihood ratio test, for statistics details see STAR methods.

(C) The viral loads of 43 individual HSCT patients with a single viral reactivation event (color-coded) against time are displayed in a three-dimension plot.

(D) Viral-load kinetic curve generated by mathematic modeling using the same set of data as shown in (C). Key parameters such as peak viral load and time as well as the three phases of CMV infection are indicated.

(E) Additional key viral kinetic parameters generated by the data modeling in (d) are presented.

reactivation occurred between d29-64 (Figure 1E). In addition, we also obtained the following important information with respect to post-HSCT CMV reactivation: (i) the median latency period for CMV replication to reach the levels of >500 copies/mL in plasma was 25 days with a minimum of 17 days and a maximum of 35 days (min-max range: 17–35 days); (ii) the median period for CMV to reach the peak level (2403.4

copies/mL) was 44 days (min-max range: 29–64 days); and (iii) the median duration of infection resulting from the first episode of CMV reactivation was 51 days (min-max range: 33–63 days) (Figure 1E).

The dynamics of cytomegalovirus-specific CD8$^+$ T-cell responses after hemopoietic stem cell transplant

To understand the dynamics of post-HSCT T-cell immune reconstitution, based on a peptide pool stimulation T-cell assay, we measured the total CMV-specific (IFNγ^+) CD8$^+$ T-cells from the blood samples of the GFPH cohorts (88 patients) collected at 280 time points over 330 days and generated a heat map (Figures 2A and S3). A likelihood ratio test of the experimental data revealed that the levels of CMV-specific CD8$^+$ T-cells produced within a window of 35 days between d50-85 were significantly higher than those observed between d15-50 ($p < 0.001$, $n = 56$) but lower than those seen between d85-120 ($p = 0.0068$, $n = 53$) (Figure 2B).

Next, we generated a CMV-specific CD8$^+$ T-cell response curve by fitting a single ordinary differential equation with the data from the 68 (out of 88) patients (Figures 2C and S4) who had at least one CD8$^+$ T-cell measurement within 180 days post-HSCT (as described in STAR methods). The response curve (Figure 2D) displayed a temporal pattern of three phases (I, II, and III) which corresponded to the three post-HSCT CMV infection phases (phase I: latency, phase II: duration of reactivation, and phase III: resolution). During phase I, the titers of the CMV-specific CD8$^+$ T-cells in most patients remained extremely low (9.1 per million PBMCs) and the median length of this phase was 20 days (range: 10–44 days) (Figure 2E). Given that the latency period for CMV viremia was 25 days (range: 17–35 days) (Figure 1E), we inferred that some CMV antigens were expressed and could stimulate T-cell response, which could be detected by our T-cell assay before CMV-DNA reached 500 copies/mL to be defined as CMV viremia, our data suggested the CD8$^+$ T-cell response commenced during or immediately after the start of CMV reactivation.

In phase II, the CMV-specific CD8$^+$ T-cells increased rapidly, eventually reaching the median level of 1055 cells/million PBMCs prior to the viral resolution phase (Figures 2D and 2E). During phase III, the levels of the CMV-specific CD8$^+$ T-cells began to plateau with a median of 1976.6 CMV-specific CD8$^+$ T-cells/million PBMCs (Figures 2D and 2E) around d180.

We also examined the dynamic changes of CMV-specific CD8$^+$ T cells for 25 patients with no detectable CMV viremia in the blood (other patients were diagnosed with single CMV viremia ($n = 50$) or repeated CMV viremia ($n = 13$)). Data showed that over time there was a significant increase in the levels of CMV-specific CD8$^+$ T-cells in these 25 patients (Figures S5A and S5B). It's probably owing to the fact that the viral load in plasma didn't meet the diagnostic (<500 copies/mL), or CMV reactivation might have occurred in tissues other than blood. Furthermore, we couldn't exclude the possibility that CMV-specific CD8$^+$T-cells were recovered by other immune mechanisms thus preventing CMV reactivation.

The dynamics of cytomegalovirus-specific CD4$^+$ T-cell responses after hemopoietic stem cell transplant

To analyze the dynamics of CMV-specific CD4$^+$ T-cell responses post-HSCT, we used the same blood samples of the GFPH cohorts (I and II) for the analysis of the CD8$^+$ T-cell responses to generate a CD4$^+$ T-cell response heatmap (Figure 3A) and perform a likelihood ratio test of CMV-specific CD4$^+$ T-cell levels over three different periods (Figure 3B). Unlike what was observed for CD8$^+$ T-cells, there was no significant difference in the CD4$^+$ levels between (d15-50], (d50-85] and (d85-d120] (Figure 3B). As in our above analysis of CD8$^+$ T-cells, 68 (out of 88) patients, who had at least one CD4$^+$ T-cell measurement within 180 days post-HSCT, were selected in the fitting of the CD4$^+$ T-cell model (Figure 3C). The frequency of responding CD4$^+$ T-cells producing IFN-γ was around 396.3 (309.2–422.6) cells/million PBMCs upon viral resolution, which was much lower than for CD8$^+$ T-cells. At d180, the mean level of virus-specific CD4$^+$ slightly decreased to 158.6 (2.54–788.5) cells/million PBMCs (Figures 3D and 3E), approximately 1/10 of those of the CD8$^+$ T-cells (Figures 2E and 3E), showing that although CMV reactivation was able to elicit a CD4$^+$ T-cell response (Wang et al., 2015), it increased during CMV viremia then declined upon suppression of the virus. The individual patient data fitting of the CD4$^+$ T-cell model was shown in Figure S6. The lower magnitude and decline after the viral resolution of CMV-specific CD4$^+$ T-cells, compared to CD8$^+$ T-cells, were further exemplified by four representative patients with multiple time points across 180 days where CD8$^+$ or CD4$^+$ T-cell counts and data fitting curves were compared (Figures S7A–S7C).

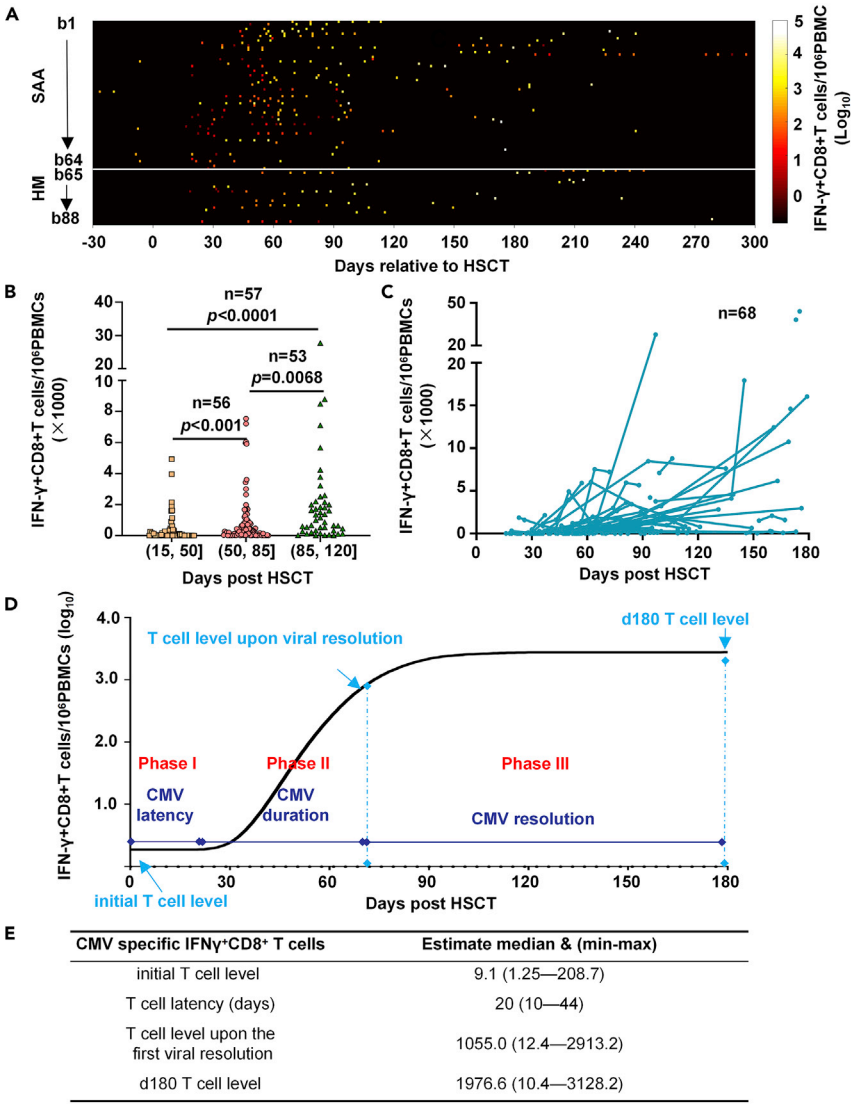

E

CMV specific IFNγ⁺CD8⁺ T cells	Estimate median & (min-max)
initial T cell level	9.1 (1.25—208.7)
T cell latency (days)	20 (10—44)
T cell level upon the first viral resolution	1055.0 (12.4—2913.2)
d180 T cell level	1976.6 (10.4—3128.2)

Figure 2. The dynamics of CMV-specific CD8⁺ T-cell responses

(A) A heatmap showing the distribution of CMV-specific CD8⁺ T-cell counts (IFN-γ⁺ CD8⁺ T-cells/10^6 PBMCs) of 88 patients (64 SAA and 24 HM cases) at various timepoints over a period of 330 days, starting 30 days before HSCT. The data are displayed with a color-coded scale from undetected level (black dots, same as the background) to $\geq 10^5$ CD8⁺ T-cells/10^6 PBMCs (white dots).

(B) The levels of CMV-specific CD8⁺ T-cells produced within three windows of 35 days (d15-50, d50-85, d85-120) are shown, for statistics details see STAR methods.

(C) Kinetic plots of 68 patients who had at least one positive datapoint within the first 90 days post-HSCT. Each line or dot represents a patient.

(D) CD8⁺ T-cell response curve generated by computational modeling using the data in (C). The three phases of the CMV-specific CD8⁺ kinetic curve which overlap with the three CMV infection stages (Figure 2D) are indicated.

(E) Additional kinetics parameters for CMV-specific CD8⁺ T-cell response, generated from data fitting in (D) are listed.

Defining an antigen-specific-CD8⁺ T-cell threshold as an indicator for cytomegalovirus containment

The demonstration of a strong correlation of the antigen-specific-CD8⁺ T-cell counts with the suppression of CMV replication and a close connection of the kinetic profiles of CMV distribution and CD8⁺ response (Figure 2D) suggested that antigen-specific CD8⁺ T-cells could be used as an indicator for CMV containment. Hence, we next sought to define a CMV-specific CD8⁺ T-cell resolution threshold for the prediction of CMV reactivation.

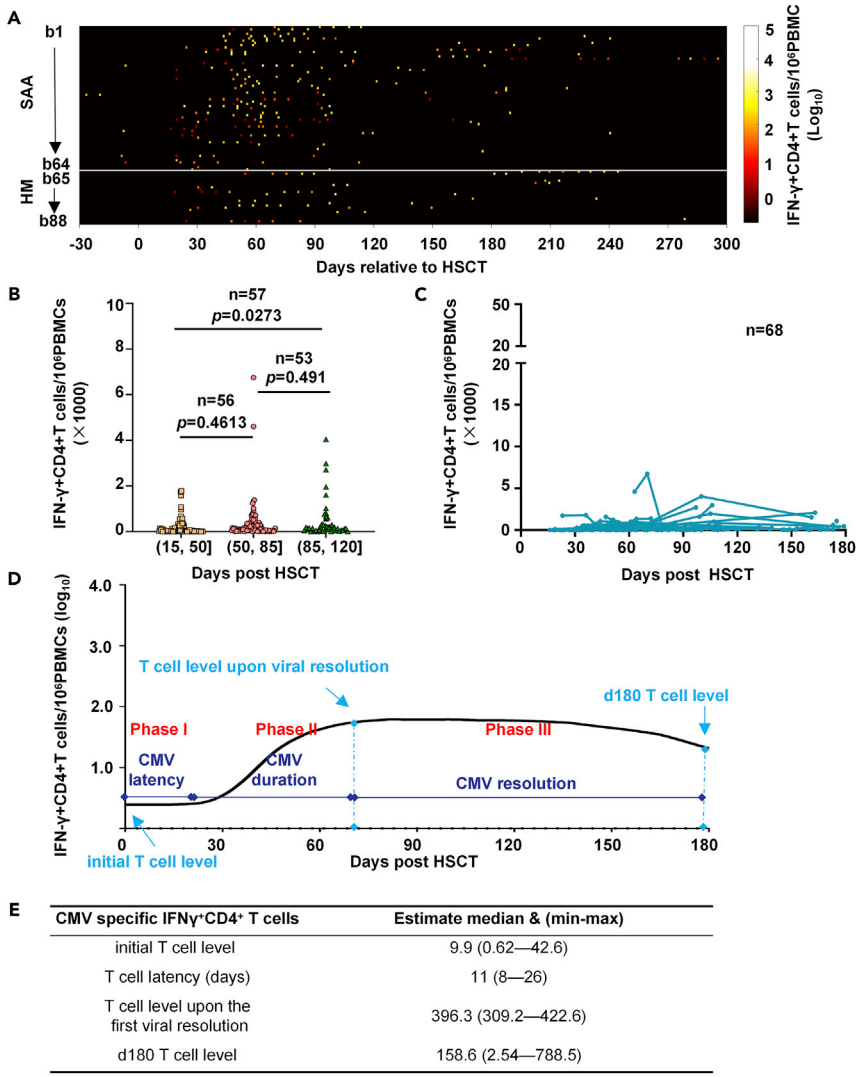

E

CMV specific IFNγ⁺CD4⁺ T cells	Estimate median & (min-max)
initial T cell level	9.9 (0.62—42.6)
T cell latency (days)	11 (8—26)
T cell level upon the first viral resolution	396.3 (309.2—422.6)
d180 T cell level	158.6 (2.54—788.5)

Figure 3. The dynamics of CMV-specific CD4$^+$ T-cell responses

(A) A heatmap displaying the distribution of CMV-specific IFN-γ$^+$ CD4$^+$ T-cells at various timepoints from 88 patients (64 SAA and 24 HM cases) over a period of 330 days before and after HSCT. The data are shown with a color-coded scale from undetected level (black dots, same as the background) to $\geq 10^5$ CD4$^+$ T-cells/10^6 PBMCs (white dots).

(B) The levels of CMV-specific CD4$^+$ T-cells produced within three windows of 35 days (d15-50, d50-85, d85-120) are shown, for statistics details see STAR methods.

(C) Kinetic plots of 68 patients who had at least one positive datapoint within the first 90 days post-HSCT. Each line or dot represents a patient.

(D) The CMV-specific CD4$^+$ T-cell response curve. The three phases of the CD4$^+$ kinetic curve and the corresponding stages of CMV infection are shown.

(E) Additional kinetic parameters of CMV-specific CD4$^+$ response are listed.

A total of 247 samples (189 from GFPH and 58 from GMUH, Tables S2–S5), with corresponding CMV-DNA and CMV-specific CD8$^+$ T-cell data, were used in a receiver operating characteristic curve (ROC) analysis to evaluate the performance of the immunological detection of CMV viremia (Figure 4). We plotted the true positive rate (sensitivity) against false-positive rate (represented as: 1-specificity). The area under the curve (AUC) calculated using the trapezoid rule (see STAR methods) was 0.727 (Figure 4A), indicating an effective measure of accuracy in using immunological detection as a diagnostic test (Hajian-Tilaki, 2013). Since this study aims to achieve a safe threshold to guide the start and end of anti-viral treatment, sensitivity is more important than specificity, therefore, we chose to concentrate on a part of the ROC curve in which the sensitivity rose sharply (0.74–0.88) without much change in specificity (0.52–0.54) (Figure 4A, indicated in the

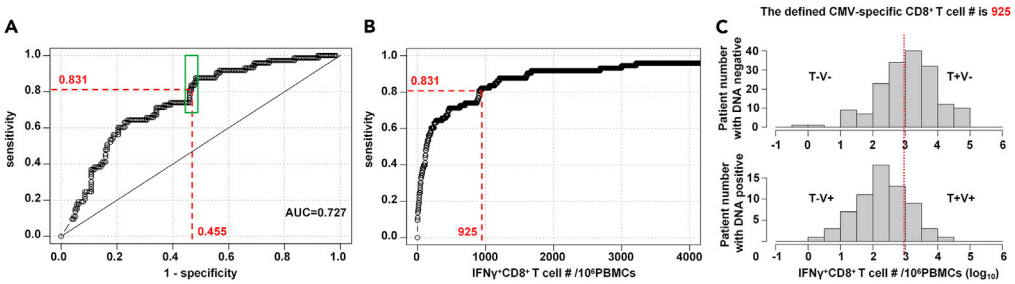

Figure 4. Defining a CMV-specific CD8$^+$ T-cell threshold for the prediction of CMV reactivation by ROC analysis

(A) A ROC with the area under the curve (AUC) value of 0.727 is shown. The portion of the ROC curve (green box) where sensitivity rises sharply (0.74–0.88) but there is little change in specificity (0.52–0.54) is used for the selection of the T-threshold. At the arbitrary detection sensitivity of 83.1%, the specificity of CMV viremia prediction is 54.5% (1–specificity = 45.5%).

(B) The T-threshold (cut-off value) at the sensitivity of 83.1% and the specificity of 54.5% is 925 IFN-γ^+ CD8$^+$ T-cells/10^6 PBMCs.

(C) Using the T-threshold value of 925 IFN-γ^+ CD8$^+$ T-cells/10^6 PBMCs, T-V-, T + V-, T-V+ and T + V+ (CMV virus titers higher than 500 copies/mL with corresponding CMV-specific CD8$^+$ T-cell counts above the T-threshold) timepoints are displayed.

green box). Within this range, multiple threshold (T) values were tested (T = 856–1153). In order to achieve a clear distinction between CMV infection and non-infection groups, we chose the sensitivity and specificity values of 83.1% and 54.5%, respectively, which gave rise to a T-threshold of 925 IFN-γ^+ CD8$^+$ T cells/10^6 PBMCs for the prediction of CMV reactivation (Figures 4A and 4B and Table S1). At this threshold, 62.8% had expected diagnostic outcomes, which included 96 T + V- timpoints (CD8$^+$ T-cells (T value) above 925 cells/10^6 PBMCs and CMV loads (V value) below 500 copies/mL) and 59 T-V+ timepoints (CD8$^+$ T-cells below 925 cells/10^6 PBMCs and CMV-DNA levels above 500 copies/mL) (Figure 4C and Tables S1–S3). In contrast, 12 of 247 timepoints showed CMV virus titers higher than 500 copies/mL with corresponding CMV-specific CD8$^+$ T-cell counts above the T-threshold (T + V+) and 80 timepoints showed no CMV viremia detected while CMV$^+$CD8$^+$ T-cells were lower than the T-threshold (T-V-) (Figure 4C and Tables S1, S4, and S5).

Based on the dynamic computational model (Figure 2D), the time to reach the threshold (925 specific CD8$^+$ T-cells/million PBMCs) was predicted to be 69 days (range: 35–112 days). Given that the presence of patients with CMV viremia following HSCT persists between d17 (the start of latency) and d98 (the sum of the longest latency period, 35 days, and the maximum duration of infection, 63 days, Figure 1E), the clearance of viral replication correlated well to the magnitude of CMV-specific CD8$^+$ T-cell response. Furthermore, our model also indicated that the median level of CMV-specific CD8$^+$ T-cell counts at the initial point of the viral resolution phase was 1055 (range: 12–2913 cells/million PBMCs) (Figures 2D and 2E).

Threshold were verified in the clinical context and showed great power in predicting the status of cytomegalovirus reactivation

To evaluate the power of T-threshold in predicting CMV reactivation clearance, we studied the kinetics of CMV-DNA and CMV-specific CD8$^+$ T-cell from multiple timepoints (Figure 5 and Tables S2–S5). Interestingly, based on a total of 155 timepoints with T+V- and T-V+, we found the CD8$^+$ T-cells were maintained above the T-threshold, at the same time, the CMV replication was effectively suppressed, in contrast, when CD8$^+$ T were lower than threshold, CMV-DNA were detected (Figure 5A and Tables S2 and S3). It showed that the defined T-threshold value reflects the switch point between CMV reactivation and CMV-specific CD8$^+$ T immunity within individual patients with HSCT (Figure 5D).

Case analyses of the 12T+V+ timepoints which comprised 4.9% of patients showed that, without the complication of a relapse of pre-HSCT disease, when patients' T-cell counts climbed above the T-threshold of 925 cells/10^6 PBMCs, their blood CMV would be cleared with a short delay of 2–9 days (Figure 5B and Table S4). Thus, the T-threshold could predict subsequent viral clearance and could be used as a safe indication index for stopping anti-viral therapy (Figure 5E).

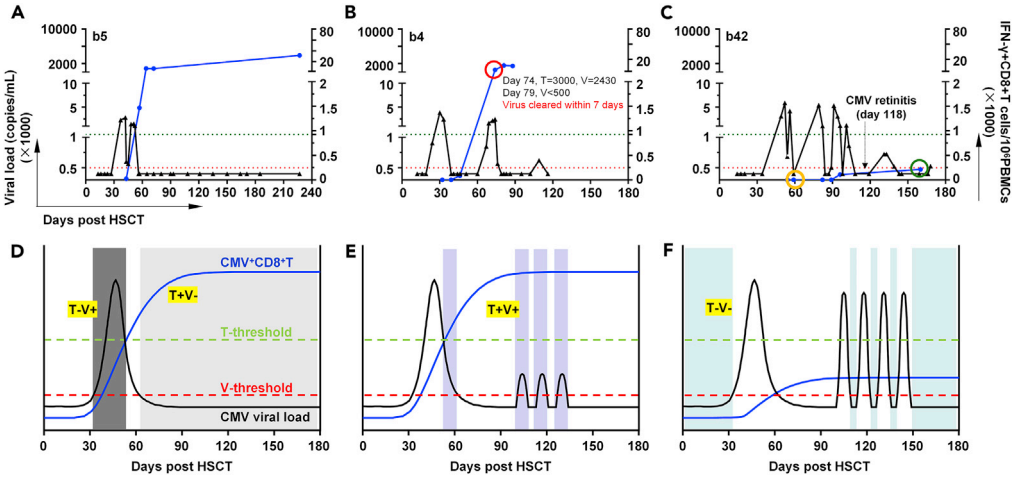

Figure 5. Representative patients and corresponding case schematic diagram

(A) Representative patient with T-V+ and T+V- timepoints showed T-threshold is a good indicator to suppress the virus.

(B) Representative patient with T+V+ timepoint (blue dot in red circle) showed the CMV reactivation can be cleared quickly if CMV $CD8^+$ T count is above T-threshold.

(C) Representative patient with T-V- timepoints within and after 90 days post-HSCT (blue dots in orange and green circles) indicated that CMV will be soon activated as long as below T-threshold.

(D) Case schematic diagram of T-V+ timepoints area (dark gray background) and T+V- timepoints area (light gray background).

(E) Case schematic diagram of T+V+ timepoints area (light purple background).

(F) Case schematic diagram of T-V- timepoints area (light blue background). Black lines: viral loads detected by quantitative RT-PCR. Blue lines or dots: CMV-specific $CD8^+$ T-cell counts measured by Flow Cytometry. Red dotted line: virological diagnostic threshold (500 copies of CMV per mL plasma). Green dotted line: immunological diagnostic threshold (925 CMV-specific $CD8^+$ T-cells per million PBMCs).

In the evaluation of post-HSCT CMV reactivation with the assistance of the T-threshold, we identified 80 T-V- timepoints (32.4%) from 37 patients (Table S5). Of them, 20 timepoints from 6 patients were found to fail to generate adequate levels of CMV-specific $CD8^+$ T-cells over a prolonged period after HSCT and suffered multiple episodes of CMV viremia (Figure 5C, blue dot in green cycle). Consequently, four of them developed CMV retinitis, above facts showed only after the establishment of adequate levels of T-cell immunity would be able to avoid further CMV infection, emphasizing the importance of using the immunological test combining CMV-DNA test in monitoring the development of post-HSCT CMV reactivation. Thus we suggested that patients with no detectable CMV viremia in the blood but with below-threshold counts of CMV-specific $CD8^+$ T-cells still require antiviral treatment (Figures 5F and 6B). For another 57 timepoints in 29 patients, T-cell immunity levels were still recovering or fluctuating below the threshold but CMV-DNA was not detected, and it occurred mostly within the first 100 days following HSCT (Figure 5C, blue dot in orange cycle). Under such circumstances, as almost all of these T-V- timepoints were seen within the period of compulsory prophylactic antiviral therapy, they would not affect post-HSCT CMV management (Figures 5F and 6B).

In sum, combining the CMV-DNA test, our threshold showed strong power in predicting the status of CMV reactivation and guiding for when to start and stop the anti-viral therapy.

DISCUSSION

Cellular immunity has long been known to play an important role in the control of CMV infection (Klenerman and Oxenius, 2016). However, to date, the dynamic interplay between CMV infection and host T-cell immunity is poorly understood. In this study, we examined the clinical characteristics of patients with HSCT from two separate medical settings and analyzed the kinetic interactions between CMV reactivation and the CMV-specific T-cell response. Owing to the very high CMV-infection rate in the Chinese population, a universal 90-day prophylactic therapy with antiviral drugs is given to all patients with HSCT. Under these conditions, the CMV viremia curve generated through analysis of blood samples of patients at various timepoints displays a typical distribution with the majority of CMV incidence occurring between d17 and d98 after HSCT and the peak of

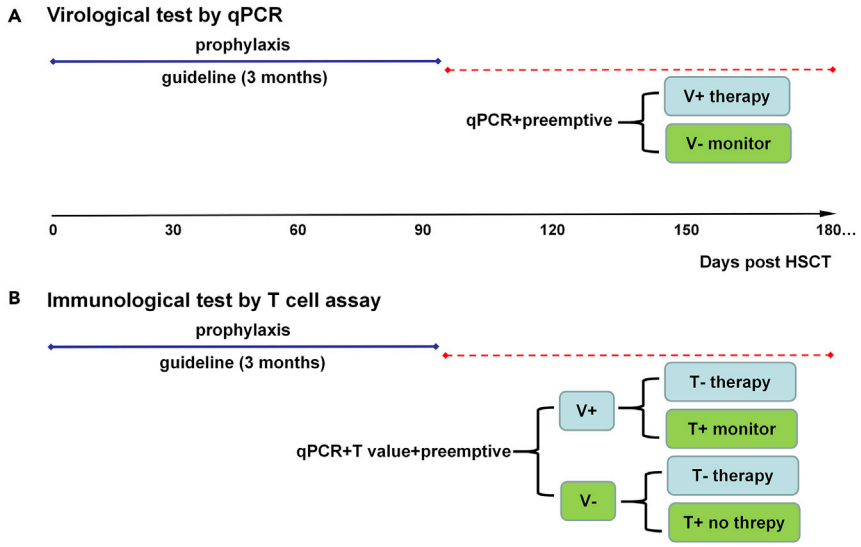

Figure 6. Therapeutic options of preemptive therapy

(A) The current preemptive approach using the virological test for monitoring.

(B) The improved preemptive approach using virological combined with immunological test for monitoring.

viral load reaching 2403.4 (958.2–30551.0) copies/mL. Notably, there is a clear association between the rise of CMV-specific $CD8^+$ T-cell response with the fall in CMV load. The latency, reactivation, and clearance of viral replication correlate with the CMV-specific $CD8^+$ T-cell response, indicating that CMV reactivation rapidly invokes a heightened and prolonged $CD8^+$ T-cell response, which in turn suppresses CMV infection into latent infection. This is consistent with previous studies (Meesing et al., 2019; Sester et al., 2002).

Although lower than the $CD8^+$ T-cell response, the synchrony of the kinetic curves of $CD4^+$ T-cells and CMV-DNA suggests that $CD4^+$ T-cells may also contribute to the inhibition of CMV replication. However, in contrast to $CD8^+$ T-cells, which remained high after 180 days, $CD4^+$ T-cell counts in a significant number of patients declined after their CMV viremia was suppressed. The different patterns of $CD4^+$ and $CD8^+$ T-cell responses may reflect the separate pathways used for the surveillance of CMV and presentation of viral antigens. It is known that $CD4^+$ T-cells predominantly recognize CMV structural proteins whereas $CD8^+$ T-cells can recognize non-structural proteins encoded by immediate-early gene loci, inhibiting CMV transcriptional reactivation before the formation of viral particles (Simon et al., 2006). In addition, the differential responses of $CD8^+$ and $CD4^+$ T-cells to post-HSCT CMV reactivation are in agreement with the view that CMV-specific $CD8^+$ T cells are more suitable to be a diagnosis indicator for suppressing CMV reactivation whereas $CD4^+$ T-cells are important for the maintenance of antiviral immunity including expansion and persistence of $CD8^+$ T-cells (Boeckh and Ljungman, 2009; Meesing and Razonable, 2018).

The ultimate application of using CMV-specific $CD8^+$ T-cell counts to the clinical prognostication of post-HSCT CMV reactivation relies on the standardization of quantification and methodologies for the evaluation of this biomarker. To this end, we used the flow cytometry intracellular cytokine staining (ICS) method to process 247 HSCT samples, then defined the $CD8^+$ T-cell counts, $\geq$925 cells/10^6 PBMCs, as the resolution threshold for CMV reactivation using ROC analysis. Recently, Messing and Razonable have reported the correlation of peripheral blood absolute lymphocyte count (PBALC) with CMV infection and proposed the PBALC value, $\leq$830/μL, as a clinically relevant threshold for the prediction of CMV infection. In addition, two other studies have demonstrated the utility of the simple and high throughput QuantiFERON-CMV assay to monitor CMV-specific $CD8^+$ T-cells for the prediction of CMV infection in patients with HSCT (Tey et al., 2013; Yong et al., 2017). However, no cut-off points for $CD8^+$ T-cell quantification were defined in these studies. Moreover, in a previous study, Angeles Clari et al. compared the performance of QuantiFERON-CMV assay with that of the ICS method and found the latter to be more sensitive in the detection of CMV-specific $CD8^+$ T-cells for patients with HSCT (Angeles Clari et al., 2012).

Our case analyses showed that CMV-specific $CD8^+$ T-cell counts were particularly useful for assessing secondary and recurrence CMV reactivation after the prophylactic period (the first 90 days post-HSCT) and that a stable reconstitution of CMV-specific T-cell immunity as measured by the continuous above-threshold levels of $CD8^+$ T-cells ensured the suppression and clearance of CMV within patients with HSCT. Even with occasional rises in viral replication, the CMV titers would decline to an undetectable level in around 7 days without the administration of antiviral drugs. On the other hand, the immune reconstitution of patients with HSCT can easily be hampered by anti-GVHD treatments or relapse of leukemia, resulting in $CD8^+$ T-cell levels below the threshold for a prolonged period. Under these circumstances, a further pre-emptive antiviral therapy is recommended to prevent CMV-associated diseases.

Patients developing CMV disease correlating with low $CD8^+$ T-cell counts, but without detectable CMV-DNA in plasma, suggesting that CMV reactivation might have occurred in distal tissues/organs and have not spilled over to blood with detectable quantity, supporting our hypothesis that the inability for the $CD8^+$ T-cells to reach the resolution threshold of 925 cells/10^6 PBMCs serves as a warning sign for CMV reactivation even in the absence of detectable levels of CMV in the plasma.

In fact, if we use $CD8^+$T cells measured after the time of prophylaxis (90 days post-HSCT) to predict viremia that comes at the same time, the sensitivity and specificity of the virological test will be 44.7% and 91.2%, which means that the rate of missed diagnosis (mistakenly to recommend withdrawal) and misdiagnosis (over-medication) of CMV-DNA test is 55.3% and 8.8% (Table S6). Traditionally, after prophylaxis treatment within 90 days post-HSCT, only the CMV-DNA test is used to monitor CMV reactivation, if CMV-DNA positive (V+), antiviral treatment continues, otherwise it stops (Figure 6A). For future CMV antiviral therapy after 90 days prophylaxis treatment, combining T-cell assay and CMV-DNA test, we want to address two exceptional circumstances (Figure 6B): 1) when CMV-DNA levels above 500 copies/mL (V+) and T-cell counts higher than T-threshold (T+) are detected after 90 days post-HSCT, the antiviral treatment is advised to stop. 2) when V- and T- are detected after 90 days post-HSCT, we strongly suggested that the antiviral therapy must be implemented although traditionally V- is considering not risky.

HSCT recipients are given prophylaxis or are closely preemptively monitored for the first 100 days after transplant in many countries (Einsele et al., 2020). Traditionally, the pre-emptive approach involves close viral load monitoring and treatment for significant viral reactivation (Figure 6A). The problem that this type of data could be applied to solving is that it becomes difficult to continue monitoring patients weekly for CMV viral load blood draws indefinitely after transplant. Thus, having a T-cell marker measured around day 90 or 100 that could predict later viremia would be quite helpful. We could use such a marker to avoid having to measure additional viral loads in patients with protective responses after the critical reactivation period.

Conclusions

The dynamic interaction between CMV virus and host immune response remains obscure, thus hindering the diagnosis and therapeutic management of patients with HSCT. In this work, we assessed the CMV reactivation kinetics and corresponding CMV antigen-specific T-cell response in individual patients, which showed that compared to CMV-specific $CD4^+$ T-cells, CMV-specific $CD8^+$ T-cells are more suitable to be a diagnostic indicator for suppressing CMV reactivation. Then, our case analyses indicated that CMV-specific $CD8^+$ T-cell counts are particularly useful for assessing CMV recurrence after the prophylactic period (the first 90 days post-HSCT) and that a stable reconstitution of CMV-specific T-cell immunity as measured by the continuous above-threshold levels of $CD8^+$ T-cells ensured the suppression and clearance of CMV within patients with HSCT. Based on ROC analysis, we defined a CMV-specific $CD8^+$ T-cell threshold (925 cells/10^6 PBMCs) for the immunological detection of CMV viremia. We addressed the utility of the T-cell threshold in two exceptional circumstances: 1) when CMV-DNA levels above 500 copies/mL (V+) and T-cell counts higher than T-threshold (T+) were detected after 90 days post-HSCT, the antiviral treatment was advised to stop. 2) when V- and T- were detected after 90 days post-HSCT, we strongly suggested that the antiviral therapy must be implemented although traditionally V- is considering not risky. Combining CMV-DNA test, our data suggest that the use of this threshold would provide more accurate guidance for prompt medication and better management of CMV infection post-HSCT.

Limitations of the study

Despite achieving several goals in defining the relationship between post-HSCT reconstitution of T-cell immunity and CMV infection, as well as the establishment of the $CD8^+$ T-threshold for predicting post-HSCT

CMV reactivation, there are limitations in this study. Owing to around 95% high prevalence of CMV infection in China, we could not validate the threshold those D-/R+ (high-risk) or even D+/R- (low-risk) patients. As a retrospective study, inconsistent timepoints over a large period of time were collected, which had to use complicated fitting mathematical model for each patient for clear interpretation, and our modeling and kinetics also could not tell the causal relationship between $CD8^+$ T-cells and CMV reactivation. Most importantly, we need to point out our T-cell assay should combine CMV-DNA test to guide only after 90 days post-HSCT, instead of a surrogate assay for the CMV-DNA test. Furthermore, this is a bi-centre investigation from one geological area. Scale-up studies with more participants from multiple clinical settings and different geological locations will improve the statistical significance of this analysis and strengthen the conclusion from our investigation.

STAR★METHODS

Detailed methods are provided in the online version of this paper and include the following:

- KEY RESOURCES TABLE
- RESOURCE AVAILABILITY
  - Lead contact
  - Materials availability
  - Data and code availability
- EXPERIMENTAL MODEL AND SUBJECT DETAILS
- METHOD DETAILS
  - Patients
  - Virological monitoring
  - Peptide pool design and preparation
  - PBMCs isolation and *ex vivo* stimulation
  - Flow cytometry
  - Mathematical modelling of viral load kinetics
  - Mathematical modeling of $CD8^+$ T-cell dynamics
  - Mathematical modeling of $CD4^+$ T-cell dynamics
- QUANTIFICATION AND STATISTICAL ANALYSIS
  - Statistical analysis for cumulative incidence curve
  - Statistical methods for exploratory data analysis
  - ROC (receiver operating characteristic curve) analysis

SUPPLEMENTAL INFORMATION

Supplemental information can be found online at https://doi.org/10.1016/j.isci.2022.105340.

ACKNOWLEDGMENTS

This work was supported by China Postdoctoral Science Foundation (2019M662863); Guangdong Basic and Applied Basic Research Foundation (2019A1515110782); Guangdong Province General Colleges and Universities Youth Innovative Talents Project (2019KQNCX120); State Key Lab of Respiratory Disease Independent Project (SKLRD-Z-202003); The grants of Guangdong-Hong Kong-Macao Joint Laboratory of Respiratory Infectious Disease (GHMJLRID-Z-202119); The grants from National Key Basic Research Project (2019YFC0810900); Ministry of Science and Technology of P.R. China (2021YFC0864400), and NSFC (81971485); Guangdong Key Basic Research Project (2019B1515120068); Guangdong Key Research and Development Project (2020B1111330001); Emergency Key Program of Guangzhou Laboratory (No. EKPG21-30-1).

AUTHOR CONTRIBUTIONS

Z.W. and J.Z. designed the experiments, analyzed data, and wrote the article; J.Z., J.C., M.Y., and Z. L. performed the experiments; P.C. established analysis modeling; W.M., R.Z., and C.W. recruited the cohort and carried out clinical treatments; J. M., J.Y., Z.C., and A.C. reviewed this work and wrote the article.

DECLARATION OF INTERESTS

The authors declare no competing financial interests.

Received: January 3, 2022
Revised: September 8, 2022
Accepted: October 7, 2022
Published: November 18, 2022

REFERENCES

Alegre, M.L. (2019). B cells, CMV, and stem cell transplant. Science *363*, 232–233. https://doi.org/10.1126/science.aav9867.

Angeles Clari, M., Munoz-Cobo, B., Solano, C., Benet, I., Costa, E., Jose Remigia, M., Bravo, D., Amat, P., and Navarro, D. (2012). Performance of the QuantiFERON-Cytomegalovirus (CMV) assay for detection and estimation of the magnitude and functionality of the CMV-Specific gamma interferon-producing CD8+ T-Cell response in allogeneic stem cell transplant recipients. Clin. Vaccine Immunol. *19*, 791–796. https://doi.org/10.1128/cvi.05633-11.

Apiwattanakul, N., Hongeng, S., Anurathapan, U., Pakakasama, S., Srisala, S., Klinmalai, C., and Andersson, B.S. (2020). CMV-Reactive NK Cells in pediatric post-hematopoietic stem cell transplant. Transplant. Proc. *52*, 353–359. https://doi.org/10.1016/j.transproceed.2019.11.010.

Berth, M., Benoy, I., and Christensen, N. (2016). Evaluation of a standardised real-time PCR based DNA-detection method (Realstar (R)) in whole blood for the diagnosis of primary human cytomegalovirus (CMV) infections in immunocompetent patients. Eur. J. Clin. Microbiol. Infect. Dis. *35*, 245–249. https://doi.org/10.1007/s10096-015-2537-0.

Boeckh, M., and Ljungman, P. (2009). How we treat cytomegalovirus in hematopoietic cell transplant recipients. Blood *113*, 5711–5719. https://doi.org/10.1182/blood-2008-10-143560.

Boeckh, M., Leisenring, W., Riddell, S.R., Bowden, R.A., Huang, M.L., Myerson, D., Stevens-Ayers, T., Flowers, M.E.D., Cunningham, T., and Corey, L. (2003). Late cytomegalovirus disease and mortality in recipients of allogeneic hematopoietic stem cell transplants: importance of viral load and T-cell immunity. Blood *101*, 407–414. https://doi.org/10.1182/blood-2002-03-0993.

Camargo, J.F., Wieder, E.D., Kimble, E., Benjamin, C.L., Kolonias, D.S., Kwon, D., Chen, X.S., and Komanduri, K.V. (2019). Deep functional immunophenotyping predicts risk of cytomegalovirus reactivation after hematopoietic cell transplantation. Blood *133*, 867–877. https://doi.org/10.1182/blood-2018-10-878918.

Cao, P., Collins, K.A., Zaloumis, S., Wattanakul, T., Tarning, J., Simpson, J.A., McCarthy, J., and McCaw, J.M. (2019). Modeling the dynamics of Plasmodium falciparum gametocytes in humans during malaria infection. Elife *8*, e49058. https://doi.org/10.7554/eLife.49058.

Chang, Y.J., Zhao, X.Y., and Huang, X.J. (2014). Immune reconstitution after haploidentical hematopoietic stem cell transplantation. Biology of blood and marrow transplantation. Biol. Blood Marrow Transplant. *20*, 440–449. https://doi.org/10.1016/j.bbmt.2013.11.028.

Chevalier, M.F., Bobisse, S., Costa-Nunes, C., Cesson, V., Jichlinski, P., Speiser, D.E., Harari, A., Coukos, G., Romero, P., Nardelli-Haefliger, D., et al. (2015). High-throughput monitoring of human tumor-specific T-cell responses with large peptide pools. OncoImmunology *4*, e1029702. https://doi.org/10.1080/2162402x.2015.1029702.

de Koning, C., Plantinga, M., Besseling, P., Boelens, J.J., and Nierkens, S. (2016). Immune reconstitution after allogeneic hematopoietic cell transplantation in children. Biology of blood and marrow transplantation. Biol. Blood Marrow Transplant. *22*, 195–206. https://doi.org/10.1016/j.bbmt.2015.08.028.

Einsele, H., Ljungman, P., and Boeckh, M. (2020). How I treat CMV reactivation after allogeneic hematopoietic stem cell transplantation. Blood *135*, 1619–1629. https://doi.org/10.1182/blood.2019000956.

Goldsmith, S.R., Slade, M., DiPersio, J.F., Westervelt, P., Lawrence, S.J., Uy, G.L., Abboud, C.N., Vij, R., Schroeder, M.A., Fehniger, T.A., et al. (2016). Cytomegalovirus viremia, disease, and impact on relapse in T-cell replete peripheral blood haploidentical hematopoietic cell transplantation with post-transplant cyclophosphamide. Haematologica *101*, E465–E468. https://doi.org/10.3324/haematol.2016.149880.

Green, M.L., Leisenring, W., Stachel, D., Pergam, S.A., Sandmaier, B.M., Wald, A., Corey, L., and Boeckh, M. (2012). Efficacy of a viral load-based, risk-adapted, preemptive treatment strategy for prevention of cytomegalovirus disease after hematopoietic cell transplantation. Biology of blood and marrow transplantation. Biol. Blood Marrow Transplant. *18*, 1687–1699. https://doi.org/10.1016/j.bbmt.2012.05.015.

Green, M.L., Leisenring, W.M., Xie, H., Walter, R.B., Mielcarek, M., Sandmaier, B.M., Riddell, S.R., and Boeckh, M. (2013). CMV reactivation after allogeneic HCT and relapse risk: evidence for early protection in acute myeloid leukemia. Blood *122*, 1316–1324. https://doi.org/10.1182/blood-2013-02-487074.

Hajian-Tilaki, K. (2013). Receiver Operating Characteristic (ROC) curve analysis for medical diagnostic test evaluation. Caspian J. Intern. Med. *4*, 627–635.

Heagy, W., Crumpacker, C., Lopez, P.A., and Finberg, R.W. (1991). Inhibition of immune functions by antiviral drugs. J. Clin. Invest. *87*, 1916–1924. https://doi.org/10.1172/JCI115217.

Hodowanec, A.C., Pikis, A., and Singer, M.E. (2020). The development of therapeutics for the treatment and prevention of CMV disease in the transplant population: a regulatory perspective. J. Infect. Dis. *221*, 109–112. https://doi.org/10.1093/infdis/jiz389.

Kamei, H., Ito, Y., Onishi, Y., Suzuki, M., Imai, H., Kurata, N., Hori, T., Tainaka, T., Uchida, H., and Ogura, Y. (2016). Cytomegalovirus (CMV) monitoring after liver transplantation: comparison of CMV pp65 antigenemia assay with real-time PCR calibrated to WHO international standard. Ann. Transplant. *21*, 131–136. https://doi.org/10.12659/aot.895677.

Klenerman, P., and Oxenius, A. (2016). T cell responses to cytomegalovirus. Nat. Rev. Immunol. *16*, 367–377. https://doi.org/10.1038/nri.2016.38.

Lee, H.Y., Rhee, C.K., Choi, J.Y., Lee, H.Y., Lee, J.W., and Lee, D.G. (2017). Diagnosis of cytomegalovirus pneumonia by quantitative polymerase chain reaction using bronchial washing fluid from patients with hematologic malignancies. Oncotarget *8*, 39736–39745. https://doi.org/10.18632/oncotarget.14504.

Liu, J., Kong, J., Chang, Y.J., Chen, H., Chen, Y.H., Han, W., Wang, Y., Yan, C.H., Wang, J.Z., Wang, F.R., et al. (2015). Patients with refractory cytomegalovirus (CMV) infection following allogeneic haematopoietic stem cell transplantation are at high risk for CMV disease and non-relapse mortality. Clin. Microbiol. Infect. *21*, 1121.e9-15. https://doi.org/10.1016/J.Cmi.2015.06.009.

Ljungman, P., Hakki, M., and Boeckh, M. (2010). Cytomegalovirus in hematopoietic stem cell transplant recipients. Infect. Dis. Clin. North Am. *24*, 319–337. https://doi.org/10.1016/j.idc.2010.01.008.

Maertens, J., and Lyon, S. (2017). Current and future options for cytomegalovirus reactivation in hematopoietic cell transplantation patients. Future Microbiol. *12*, 839–842. https://doi.org/10.2217/fmb-2017-0095.

Meesing, A., Abraham, R.S., and Razonable, R.R. (2019). Clinical correlation of cytomegalovirus infection with CMV-specific CD8+T-cell Immune competence score and lymphocyte subsets in solid organ transplant recipients. Transplantation *103*, 832–838. https://doi.org/10.1097/tp.0000000000002396.

Meesing, A., and Razonable, R.R. (2018). Absolute lymphocyte count thresholds: a simple, readily available tool to predict the risk of cytomegalovirus infection after transplantation. Open Forum Infect. Dis. *5*, ofy230. https://doi.org/10.1093/ofid/ofy230.

Moss, P., and Rickinson, A. (2005). Cellular immunotherapy for viral infection after HSC transplantation. Nat. Rev. Immunol. *5*, 9–20. https://doi.org/10.1038/nri1526.

Pei, X.Y., Zhao, X.Y., Xu, L.P., Wang, Y., Zhang, X.H., Chang, Y.J., and Huang, X.J. (2017). Immune reconstitution in patients with acquired severe aplastic anemia after haploidentical stem cell transplantation. Bone Marrow Transplant. *52*, 1556–1562. https://doi.org/10.1038/bmt.2017.174.

Piray, P., Dezfouli, A., Heskes, T., Frank, M.J., and Daw, N.D. (2019). Hierarchical Bayesian inference for concurrent model fitting and comparison for group studies. PLoS Comput. Biol. *15*, e1007043. https://doi.org/10.1371/journal.pcbi.1007043.

Rogers, R., Saharia, K., Chandorkar, A., Weiss, Z.F., Vieira, K., Koo, S., and Farmakiotis, D. (2020). Clinical experience with a novel assay measuring cytomegalovirus (CMV)-specific CD4+and CD8+T-cell immunity by flow cytometry and intracellular cytokine staining to predict clinically significant CMV events. BMC Infect. Dis. *20*, 58. https://doi.org/10.1186/s12879-020-4787-4.

Sellar, R.S., and Peggs, K.S. (2012). Therapeutic strategies for the prevention and treatment of cytomegalovirus infection. Expert Opin. Biol. Ther. *12*, 1161–1172. https://doi.org/10.1517/14712598.2012.693471.

Sester, M., Sester, U., Gärtner, B.C., Girndt, M., Meyerhans, A., and Köhler, H. (2002). Dominance of virus-specific CD8 T cells in human primary cytomegalovirus infection. J. Am. Soc. Nephrol. *13*, 2577–2584. https://doi.org/10.1097/01.asn.0000030141.41726.52.

Simon, C.O., Holtappels, R., Tervo, H.-M., Böhm, V., Däubner, T., Oehrlein-Karpi, S.A., Kühnapfel, B., Renzaho, A., Strand, D., Podlech, J., et al. (2006). CD8 T cells control cytomegalovirus latency by epitope-specific sensing of transcriptional reactivation. J. Virol. *80*, 10436–10456. https://doi.org/10.1128/jvi.01248-06.

Simons, L., Cavazzana, M., and André, I. (2019). Concise Review: boosting T-cell reconstitution following allogeneic transplantation-current concepts and future perspectives. Stem Cells Transl. Med. *8*, 650–657. https://doi.org/10.1002/sctm.18-0248.

Tey, S.-K., Kennedy, G.A., Cromer, D., Davenport, M.P., Walker, S., Jones, L.I., Crough, T., Durrant, S.T., Morton, J.A., Butler, J.P., et al. (2013). Clinical assessment of anti-viral CD8+T cell immune monitoring using QuantiFERON-CMV (R) assay to identify high risk allogeneic hematopoietic stem cell transplant patients with CMV infection complications. PLoS One *8*, e74744. https://doi.org/10.1371/journal.pone.0074744.

van den Brink, M.R.M., Velardi, E., and Perales, M.A. (2015). Immune reconstitution following stem cell transplantation. Hematology. Am. Soc. Hematol. Educ. Program *2015*, 215–219. https://doi.org/10.1182/asheducation-2015.1.215.

Wagner-Drouet, E., Teschner, D., Wolschke, C., Janson, D., Schäfer-Eckart, K., Gärtner, J., Mielke, S., Schreder, M., Kobbe, G., Kondakci, M., et al. (2021). Standardized monitoring of cytomegalovirus-specific immunity can improve risk stratification of recurrent cytomegalovirus reactivation after hematopoietic stem cell transplantation. Haematologica *106*, 363–374. https://doi.org/10.3324/haematol.2019.229252.

Wang, Z., Wan, Y., Qiu, C., Quiñones-Parra, S., Zhu, Z., Loh, L., Tian, D., Ren, Y., Hu, Y., Zhang, X., et al. (2015). Recovery from severe H7N9 disease is associated with diverse response mechanisms dominated by CD8(+) T cells. Nat. Commun. *6*, 6833. https://doi.org/10.1038/ncomms7833.

Wang, Z., Yang, X., Zhong, J., Zhou, Y., Tang, Z., Zhou, H., He, J., Mei, X., Tang, Y., Lin, B., et al. (2021). Exposure to SARS-CoV-2 generates T-cell memory in the absence of a detectable viral infection. Nat. Commun. *12*, 1724. https://doi.org/10.1038/S41467-021-22036-Z.

Yong, M.K., Cameron, P.U., Slavin, M., Morrissey, C.O., Bergin, K., Spencer, A., Ritchie, D., Cheng, A.C., Samri, A., Carcelain, G., et al. (2017). Identifying cytomegalovirus complications using the Quantiferon-CMV assay after allogeneic hematopoietic stem cell transplantation. J. Infect. Dis. *215*, 1684–1694. https://doi.org/10.1093/infdis/jix192.

STAR★METHODS

KEY RESOURCES TABLE

REAGENT or RESOURCE	SOURCE	IDENTIFIER
Antibodies		
LIVE/DEAD Fixable Aqua	Thermo	Cat# L34957
anti-CD3-FITC	BD	Cat# 561802; clone HIT3a; RRID:AB_10893003
anti-CD4-APC-H7	BD	Cat# 560158; clone RPA-T4; RRID:AB_1645478
anti-CD8-PerCPCy5.5	BioLegend	Cat# 344710; clone SK1; RRID:AB_2044010
anti-IFNγ-APC	BD Pharmingen™	Cat# 554702; clone B27; RRID:AB_398580
Biological samples		
Peripheral blood of HSCT patients	Guangzhou First People's Hospital	N/A
Peripheral blood of HSCT patients	First Affiliated Hospital of Guangzhou Medical University	N/A
Chemicals, peptides, and recombinant proteins		
Ficoll-Paque	GE Healthcare	Cat# 17-1440-03
RPMI 1640 medium	Gibco	Cat# C11875500BT
FBS	Biological Industries	Cat# 04-001-1ACS
penicillin-streptomycin	Gibco	Cat# 15140122
rIL-2	ROCHE	Cat# 11147528001
GolgiPlug	BD Biosciences	Cat# 555029
Cytofix and Perm	BD Bioscience	554714
HCMV pp65, IE-1 and IE-2 peptides	GL Biochem	N/A
Critical commercial assays		
DNA Blood Mini Kit	Qiagen	Cat#51104
Human Cytomegalovirus Fluorescent Polymerase Chain Reaction Diagnostic Kit	Da An Gene CO., Ltd. of Sun Yat-Sen University	Cat#DA0123
Deposited data		
Raw and analyzed data	Baidu Netdisk	https://pan.baidu.com/disk/main?from=homeFlow#/index?category=all
Software and algorithms		
R (version 3.2.3)	R project	https://www.r-project.org
FlowJo V10	BD Bioscience	https://www.bdbiosciences.com/en-ca/products/software/flowjo-v10-software
GraphPad prism 7.00	GraphPad Software	https://www.graphpad-prism.cn/
Other		
FACSAria III instrument	BD Bioscience	64828217
Prism Fluorescent quantitative PCR instrument ABI 7500	ABI	275009018

RESOURCE AVAILABILITY

Lead contact

Further information and requests for resources and reagents should be directed to and will be fulfilled by the lead contact, Zhongfang Wang (wangzhongfang@gird.cn).

Materials availability

There are restrictions to the availability of peptides pool due to intellectual property protection.

Data and code availability

Data or additional information reported in this paper is available from the lead contact upon request. The original computer code is publicly available at https://github.com/axin43/CMV-modelling. Any additional information required to reanalyze the data reported in this paper is available from the lead contact upon request.

EXPERIMENTAL MODEL AND SUBJECT DETAILS

109 HCMV-seropositive patients who had undergone allogeneic HSCT were enrolled in this study. Patient characteristics are shown in Table 1. This study was approved by the Ethics Commission of the First Affiliated Hospital of Guangzhou Medical University (No.2020–51).

METHOD DETAILS

Patients

109 HCMV-seropositive patients who had undergone allogeneic HSCT were enrolled in this study. Blood samples were collected from 88 patients in Guangzhou First People's Hospital (GFPH, Cohort I & II) to build mathematical models. Later, an additional 21 patients in the First Affiliated Hospital of Guangzhou Medical University (GMUH, Cohort III) combined with 58 patients from Cohort I & II were used to determine and validate the T-threshold. Patient characteristics are shown in Table 1. This study was approved by the Ethics Commission of the First Affiliated Hospital of Guangzhou Medical University (No.2020–51).

Virological monitoring

Viral DNA was purified from blood samples using the Qiagen DNA Blood Mini Kit (Cat#51104). CMV-DNA was quantified with the ABI 7500 Prism Fluorescent quantitative PCR instrument using the Human Cytomegalovirus Fluorescent Polymerase Chain Reaction Diagnostic Kit (Cat#DA0123, Da An Gene CO., Ltd. of Sun Yat-Sen University) according to the manufacturer's instructions and performed at the hospital laboratory departments. The diagnostic threshold was 500 DNA copies/mL.

Peptide pool design and preparation

CMV-specific peptides were designed and synthesized as follows: 383 overlapping 15-amino acid peptides spanning the entire proteins of the HCMV pp65, IE-1 and IE-2 with 11 overlapping residues between neighboring peptides were generated with an online peptide generator (Peptide 2.0), and were synthesized by GL Biochem Corporation (Shanghai) with a purity of over 80%. Each peptide was dissolved in DMSO, and pooled with each at a concentration of 1 μM to form a stock.

PBMCs isolation and *ex vivo* stimulation

Peripheral blood mononuclear cells (PBMCs) were isolated from heparinized whole blood by density-gradient sedimentation using Ficoll-Paque according to the manufacturer's instructions (GE Healthcare, 17-1440-03). 5×10^5 PBMCs were cultured in RPMI 1640 medium (Gibco) supplemented with 10% heat inactivated FBS (Biological Industries, Israel Beit-Haemek), 100 U/mL penicillin (Gibco) and 0.1 mg/mL streptomycin (Gibco). The PBMCs were treated with the peptide pool containing 383 15-mer peptides at 250 nM/each peptide in the presence of 20 U/mL rIL-2 and 1 μM GolgiPlug (BD Biosciences, San Diego, CA) overnight at 37°C, 5% CO_2 (Wang et al., 2021). The approach of using a large peptide pool to stimulate PBMCs was based on that developed by Chevalier et al. and was previously validated for CMV peptides (Chevalier et al., 2015).

Flow cytometry

Cells harvested from the overnight stimulation cultures were washed and incubated with LIVE/DEAD Fixable Aqua (1:1000, Thermo, Cat# L34957) for 15 min on ice. Cells were then washed again and surface-stained for 30 min on ice with the following antibodies: anti-CD3-FITC (1:200, BD, clone HIT3a, Cat# 561802), anti-CD4-APC-H7 (1:200, BD, clone RPA-T4, Cat# 560158), anti-CD8-PerCPCy5.5 (1:100, BioLegend, clone SK1, Cat# 344710). After fixation and permeabilization with Cytofix and Perm (BD Bioscience, Cat# 554714) on ice for 15 min, intracellular staining (ICS) was performed on ice for 30 min with anti-IFNγ-APC (1:100, BD Pharmingen™, clone B27, Cat# 554702). The samples were acquired using an FACSAria III instrument (BD Bioscience) and analyzed with FlowJo software (Treestar).

Mathematical modelling of viral load kinetics

In order to quantify the kinetics of the first wave of infection, we fit a mathematical model to the CMV patients' viral load data (using Bayesian hierarchical inference). We chose the patients exhibiting a relatively strong viral shedding (having at least two DNA values lager than the detection limit of 500 and having at least one DNA value larger than 1000 within 90 days post-HSCT). We also excluded any patient showing reoccurrence within 90 days post-HSCT (defined by the occurrence of >500 value following at least two negative examinations after the first wave of infection within 90 days post-HSCT). Hence, 43 (out of 88) patients were selected in the fitting of the viral load model. The viral load model is a single ordinary differential equation,

$$\frac{dV}{dt} = p_V\left(\frac{t^9}{t^9 + L_{V1}{}^9}\right)\left(\frac{L_{V2}{}^9}{t^9 + L_{V2}{}^9}\right)V + c(V_0 - V), \qquad \text{(Equation 1)}$$

where p_V is the maximum growth rate and c is the viral clearance rate. The two sigmoidal functions $t^9/(t^9+L_{V1}{}^9)$ and $L_{V2}{}^9/(t^9+L_{V2}{}^9)$ phenomenologically model a possibly delayed viral reactivation and an inhibitory effect on viral growth respectively. Lv_1 and Lv_2 can be seen as the latency of activation and the latency of inactivation respectively when the power coefficients of the sigmoidal functions in the phenomenological models are relatively large (Note that the extreme case is the sigmoidal functions will become discontinuous stepwise functions when the power goes to infinity, with latencies Lv_1 and Lv_2; but for computational efficiency, we need a finite power to warrant smoothness of the functions). We chose a power of 9 which gave sufficiently steep transitions between the minima and the maxima in the sigmoidal functions without introducing difficulty in numerical integration.

Note that the model that can phenomenologically capture the clinical data is not unique and Equation 1 is just one choice with a simple structure. V_0 is the initial viral load (i.e., $V(0)$). Bayesian hierarchical inference, is a well-established statistical method for parameter estimation used to study kinetics of many other diseases (Cao et al., 2019; Piray et al., 2019), was used to fit the mathematical model to data. The method generates many samples (4000 in our study) from the posterior distribution of model parameters, which are used to produce the model-predicted time series of viral load curves for individual patients (time series predictions are shown by predicted median and 95% Prediction intervals (PI) of the viral load). Median predictions and 95% PI of several key infection-related quantities, such as peak viral load, peak time, latency and duration, are calculated based on the predicted median curves of the viral load. Model fitting was implemented in R (version 3.2.3) and Stan (version 2.17.0) and computer code is publicly available at (GitHub link).

Mathematical modeling of CD8$^+$ T-cell dynamics

68 (out of 88) patients, who had at least one CMV$^+$ CD8$^+$ T-cell measurement within 180 days post-HSCT, were selected in the fitting of the CD8$^+$ T-cell model, which is a single ordinary differential equation.

$$\frac{dT}{dt} = p_T\left(\frac{t^9}{t^9 + L_T{}^9}\right) + d(T_0 - T), \qquad \text{(Equation 2)}$$

where p_T is the maximum growth rate and d is the decay rate. We use a sigmoidal function $t^9/(t^9+L_T{}^9)$ to phenomenologically model a delayed activation of CD8$^+$ T-cells. T_0 is the initial CD8$^+$ T-cell level after HSCT and $T(0) = T_0$.

The method for model fitting is the same as that for viral load data fitting. Based on the model-predicted time series curves of CD8$^+$ T-cells, we calculate four quantities of interest that characterise the kinetics of CD8$^+$ T-cells: initial T-cell level (the CD8$^+$ T-cell level immediately after HSCT), latency (the time before CD8$^+$ T-cell level reaches above 10% of the initial level), d180 T-cell level (the CD8$^+$ T-cell level at 180 days post-HSCT) and CD8$^+$ T-cell level upon the first viral resolution.

Mathematical modeling of CD4$^+$ T-cell dynamics

68 (out of 88) patients, who had at least one CMV$^+$ CD4$^+$ T-cell measurement within 180 days post-HSCT, were selected in the fitting of the CD4$^+$ T-cell model. The CD4$^+$ T-cell model takes a similar form to that of CMV-DNA.

$$\frac{dT}{dt} = p_T\left(\frac{t^9}{t^9 + L_{T1}{}^9}\right)\left(\frac{L_{T2}{}^9}{t^9 + L_{T2}{}^9}\right)T + d(T_0 - T), \qquad \text{(Equation 3)}$$

where p_T is the maximum growth rate and d is the decay rate. T_0 is the initial $CD4^+$ T-cell level after HSCT and $T(0)=T_0$.

We calculate four quantities of interest that characterise the kinetics of $CD4^+$ T-cells: initial T-cell level: the $CD4^+$ T-cell level immediately after HSCT; T-cell latency: the time before T-cell level reaches above 10% (this value is provisional) of the initial level; d180 T-cell level: the $CD4^+$ T-cell level at 180 days post-HSCT; $CD4^+$ T-cell level upon the first viral resolution.

QUANTIFICATION AND STATISTICAL ANALYSIS

Statistical analysis for cumulative incidence curve

Log-rank (Mantel-Cox) test was applied in cumulative incidence curve comparison between different cohorts.

Statistical methods for exploratory data analysis

Since the clinical data include longitudinal measurements of CMV-DNA and T-cells grouped by patients, nested linear mixed-effects modelling was used to determine if a quantity of interest, such as CMV-DNA (viral load) and CMV-specific $CD8^+$ and $CD4^+$ T-cells, exhibits a significantly higher or lower level in one period of time than that in another period of time (e.g., 0–30 days vs. 30–60 days post-HSCT). The linear model we used was:

$$Q = a_0 + a_1 T + a_2 + \varepsilon, \quad \text{(Equation 4)}$$

where Q is the predicted value of the quantity of interest, which is assumed to be a linear function of the patient-independent fixed effect (i.e., the term a_0+a_1T), the patient-specific random effect on the predicted quantity (i.e., the term a_2) and the random effect of the measurement error (i.e., the term ε). T takes either 1 or 2 to indicate different periods of time. Statistical significance was indicated by the p value, which was obtained by a likelihood ratio test (LRT) between the linear model Equation 4 and its associated model where period-dependency was removed:

$$Q = a_0 + a_2 + \varepsilon, \quad \text{(Equation 5)}$$

We set a significance level of 0.05 for our study and a p value less than 0.05 leads to rejection of the null hypothesis of period-independency assumed in Equation 5 and therefore indicates a statistically significant difference in the quantity of interest between the examined two periods of time. In the results, we reported the p values and the mean estimates of parameter a_1 in Equation 4 as the statistical evidence to show whether a quantity of interest in one period of time was significantly higher/lower than that in another period of time.

ROC (receiver operating characteristic curve) analysis

The CMV virological test (qPCR) and immunological test (CMV-specific IFN-γ producing T-cell) were not always performed on the same day. Under such circumstances, CMV-DNA data closest to, and always within ± 3 days of, the immunological detection time point were selected for ROC analysis. In this way, we obtained 247 pairs of CMV-DNA and T-cell data points for the ROC analysis. The analysis was implemented in R (version 3.2.3) and computer code is publicly available at https://github.com/axin43/CMV-modelling.